National University of Science and Tehcnology "POLITEHNICA" Bucharest
University Center of Pitesti
Faculty of Mechanics and Technology

SCIENTIFIC BULLETIN
AUTOMOTIVE series
year XXIX, no. 33

ANALYSIS OF POROSITY EVOLUTION IN A BONDED ASSEMBLY UNDER TENSILE-SHEAR STRESS BY X-RAY MICROTOMOGRAPHY

Andreea TINTATU*, Claudiu BADULESCU[1]

[1] ENSTA Bretagne, UMR CNRS 6027, IRDL, F-29200, Brest, France

*Corresponding author e-mail andreea.tintatu@yahoo.com

Article history
Received 01.07.2023
Accepted 14.10.2023

DOI https://doi.org/10.26825/bup.ar.2023.001

Abstract. In the technical field of bonded assemblies, one of the main defects that can accompany adhesive joints is the presence of porosities. In this paper, the results obtained from the characterisation of the distribution of porosities in the adhesive joint using X-ray µ-tomography and the evolution of this distribution during the mechanical loading of the joint were highlighted. The aim of this work was therefore to post-process the tests performed using an X-ray µ-tomograph and to find the evolution of several parameters (porosity rate, evolution of the geometric shape of the porosities, etc.) as a function of the load applied.
Keywords: bonded joint, structural assemblies, pores, X-ray µ-tomography, analysis tool.

INTRODUCTION

In the design and manufacture of structures, the assembly of components is a crucial step in terms of durability and reliability. For many years, mechanical assembly techniques such as bolting, riveting and welding have been the traditional ones. However, these techniques are often very difficult or impossible to put into practice due to the very complex structures of the assemblies or the nature of the materials. Therefore, alternative techniques such as structural bonding have been developed to offer solutions much easier to use than traditional assembly techniques, and to ensure that the process is well controlled. The technique of assembling materials based on the use of adhesives is gradually gaining ground over time in numerous industrial applications such as naval, automotive and aerospace. Structural assemblies are defined as assemblies whose mechanical strength is sufficiently high and close to that of the structure itself [1]. However, these assembled joints are currently not completely mastered in terms of characterization of the mechanical behaviour [2], even less in terms of the effect of defects on the mechanical behaviour. These families of defects can appear during the bonding phase. One of the main defects that accompanies assembled joints is represented by the presence of the porosities. As the porosities are structural defects, the hypothesis that they influence the mechanical properties of the material seems reasonable. In general, these porosities, encountered for two-component adhesives, are generated when mixing these components and amplificated during the curing phase.
To better understand the relationship between material properties and its microstructure including defects, it is necessary to obtain images of these features and analyse them quantitatively (number, size, volume fraction, connectivity, etc.). Thanks to microscopy, it is possible to obtain 2D images of these features, whatever their size: the optical microscope is used for features larger than 1 µm, while electron microscopes (scanning electron microscope, SEM or transmission electron microscope, TEM) are used for smaller elements down to the nanoscale [3]. However, these techniques are destructive (the material must be sectioned) and only provide 2D images on which certain parameters cannot be determined: for example, the number of elements and their possible connectivity require 3D images. Thanks to X-ray

µ-tomography it is possible to overcome these difficulties. X-ray µ-tomography can cover a wide range of observations of microstructural defects with the added advantage of being non-destructive [4].
X-ray µ-tomography offers the possibility of recording multiple scans of a sample in which the experimental environment (stress state, temperature, etc.) changes over time. The result obtained is a series of 3D images of the internal microstructure of the material as a function of time [5]. Such experiments generally provide unique data, essential for testing existing models or developing new ones. Although the very first 3D images obtained by researchers were sometimes processed manually, the development of 3D imaging software (e.g. ImageJ - [6], Aviso - [7], Vgstudio - [8]) has greatly promoted semi-automatic to automatic processing. On the basis of such software or homemade codes, 3D images can be used quantitatively and, for example, they can now be transformed directly into 3D meshes used for finite element calculations or other numerical models [9].
Therefore, the tests analysed were performed as part of the thesis of V. Dumont [10] and the present study focuses on the micrometric analysis of bonded joints (epoxy adhesive and aluminium alloy) with the main objective of obtaining the conditions of influence of porosity on these assemblies by identifying the 3D microstructure of the adhesive after the polymerization process (identification of phases in the adhesive, their distribution).

MATERIAL AND EXPERIMENTAL METHODS

Sample preparation

The geometry of the samples must respect two criteria to remain in the framework of our study: they must be bonded assemblies and their dimensions must be adequate for the resolution of the X-ray microtomography measurements. To verify these requirements, the specimens shown in Figure 1 will be used.
The analysis of the effect of porosities was performed on an epoxy type adhesive. The samples consist of two aluminium substrates (2017A) bonded by a layer of epoxy resin of given thickness. In addition, threaded holes are provided at each end of the specimens for installation in the device for tensile-shear testing by X-ray tomography (Figure 1).

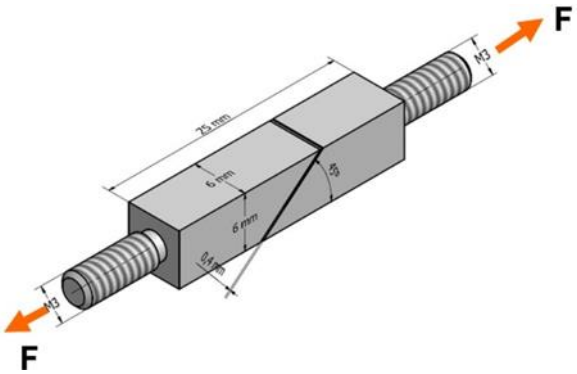

Figure 1. The geometry of the samples

The thickness of the adhesive is set at 400 µm and it is controlled by a spacer system [11]. The system used in the manufacture of the samples, consisting of a rake-like configuration (Figure 2a) and the special bonding device (Figure 2b), is illustrated in Figure 2. This system enables both the control of adhesive thickness and the correct alignment of substrates. Threaded holes are also used during the bonding process to control the relative positioning of substrates.
For proper adhesion between the adhesive layer and the substrates, a conventional surface treatment (chemical and mechanical) is carried out on the bonding surfaces to eliminate any fatty by-product which may remain after the machining of the substrates and create an adequate surface roughness for the desired mechanical interlock between substrates and adhesive. The adhesive joint is then prepared by applying the mixture of epoxy resin and hardener to the two substrates assembled and installed in the device (Figure 2b) adjusted to obtain the desired joint thickness. Finally, the samples are placed in a

Secasi Technologies ™100/60 thermal chamber at 115°C for 1 hour to provide a completely cured material.

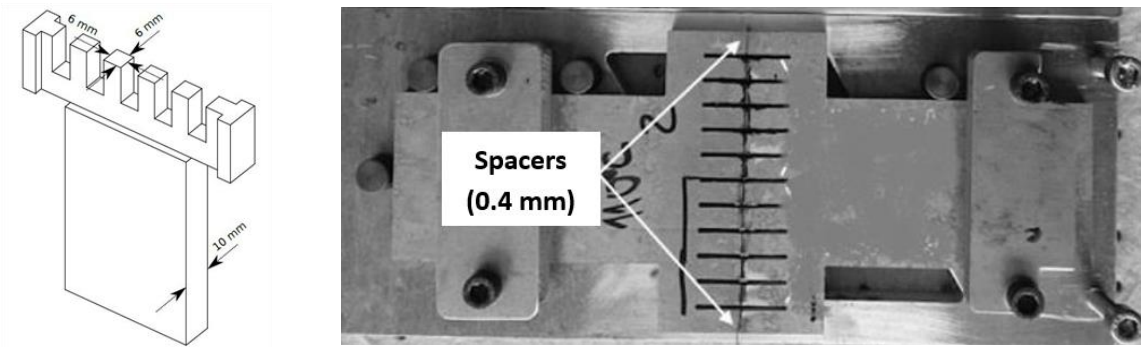

(a) Machining of samples

(b) Sample mounted in the bonding apparatus with controlled joint thickness

Figure 2. Controlled sample fixation and bonding system

X-ray µ-tomography setups

The methodology used to perform the tomographic acquisitions (Figure 3) can be briefly described as follows [12]:

- An X-ray beam is sent through an object positioned on a motorized stage, which rotates at an angular step depending on the number of X-ray images required;
- A scintillator placed upstream of the detector will convert the X-ray photon radiation into photons in the visible range;
- A camera equipped with a detector (classically a Charge-Coupled Device detector) records a 2D X-ray for each position between 0 and 180° (or 360°);
- In addition to the radiographs of the object, references (radiographs without a sample corresponding to the incident beam) and black images (zero flux signal from the sensor) are recorded;
- All of the x-rays are then processed by a mathematical algorithm;
- The reconstruction makes it possible to obtain in the form of a volume the three-dimensional mapping of the local values of the linear absorption coefficient of X-ray radiation.

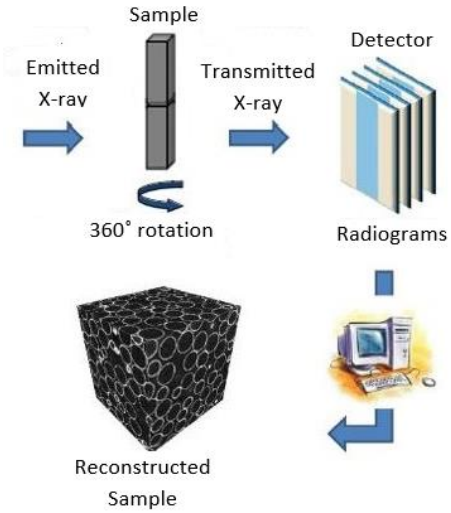

Figure 3. Principle of tomography

As mentioned earlier, X-rays are generated during acquisition. From this set of radiographs, to which references and zero-flux images are associated, we obtain projections of the attenuation constant μ

considered as a continuous function of three spatial variables (x, y, z), which can be calculated as follows:

$$\frac{I}{I_0} = \exp\left(\int \mu(x,y,z)dx\right) \quad (1)$$

Where:

- I_0 represents the intensity of the source;
- I is the detected intensity;
- $\boldsymbol{x}$ represents the distance along the transmission path.

The 3D structure of the reconstructed sample is defined with a given voxel size, in the same way as the pixels that make up an image. This voxel size is linked to the spatial resolution of the measurement, but is not equivalent. In this case, a relationship can be established between these quantities, with the spatial resolution becoming twice as large as the voxel [13]. However, the spatial resolution of the experimental configuration also depends on various external parameters relating to the test set. In view of the importance of these external parameters, the samples were tested in situ to obtain a tomography less influenced by these conditions. However, this type of experiment is difficult to handle due to the measurement artifacts it can produce. Our aim is to find a simple method for analysing the results obtained by 3D reconstruction while minimizing the influence of these artifacts.
The samples are placed in a *Phoenix VtomeX tomograph* equipped with a *Varian* X-ray detector *Paxscan ™*offering a resolution of 1920x1536 pixels. This detector emits a 14-bit coded grayscale image of the attenuation. The tomograph chamber includes a 3 kN traction machine, which allows X-ray tomography measurements to be performed while applying a mechanical load to the sample (Figure 4).

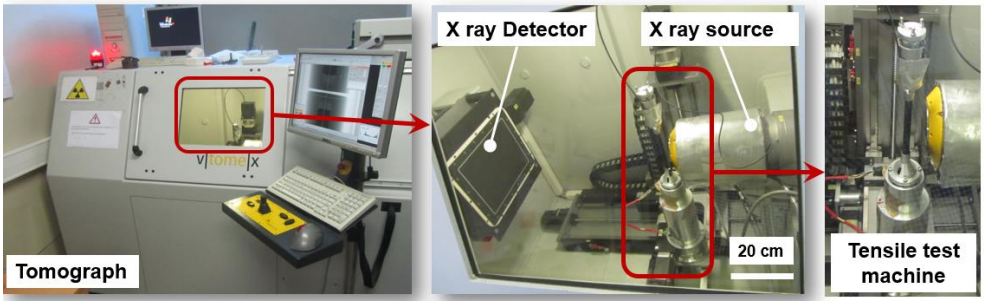

Figure 4. The laboratory *Phoenix VtomeX* tomograph

The voxel size obtained using this experimental setup is 4.5 µm x 4.5 µm x 4.5 µm. The corresponding spatial resolution should be consistent with the characteristic size of the porosities to be observed. It will be assumed that the measurements occur for a quasi-static state of the samples and that, therefore, the corresponding characteristic time obscures the acquisition time for a series of radiographs. The experimental set-up is therefore well suited to the measurements to be performed. To reconstruct the observed volume in its entirety, the acquisition is carried out with a rotational movement of the sample. As already mentioned, the tensile testing machine included in the scanner allows these measurements to be performed while applying mechanical load to the samples. The test was carried out by gradually increasing the applied load with a step of 170 N (Figure 5). The ramps between the steps are controlled by displacement (0.5 mm / min). The process continues until the sample fails.

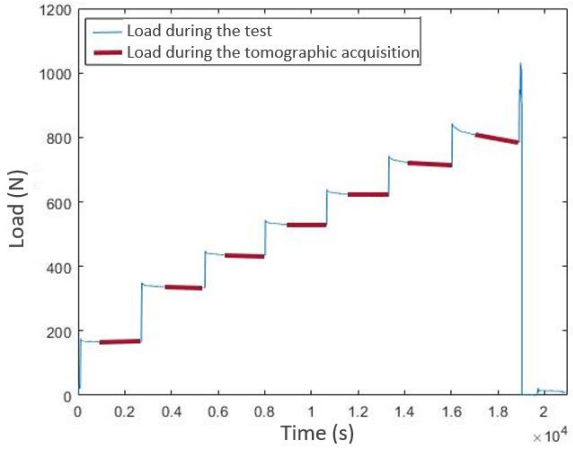

Figure 5. Load applied on samples

Post-processing of tomographic data

A time series of sets of radiographs is provided by the experiments detailed above. The shape of the reconstructed volumes is a matrix of 2000x200x1500 voxels^3 under tensile-shear load. They are cut to retain only the area of interest (the adhesive joint and a small part of the substrates, Figure 6). To facilitate the analysis, only the central part of the samples was reconstituted. The tensile-shear specimen is difficult to analyse because the central volume reconstructed is very large and cannot be analysed with a standard computer calculation tool. The solution found to reduce this volume, illustrated in Figure 6, is to rotate the reconstructed tomographic volume through an angle of 45° in order that the plane of the assembled joint is at an angle of 0° to the horizontal. This schematic representation of the central part of the sample (Figure 7a) is constituted from raw grayscale images which display 2 visible phases (see Figure 7b to Figure 7d): the adhesive and the porosities.
The raw data obtained by X-ray tomography was then post-processed to extract the following information: the spatial distribution and ratio of each phase and their evolution during the different loads applied. The complete study of the microstructure in relation to the load applied required the development of a processing tool that:

- Removes artefacts from reconstructed adhesive slices and extracts the mean intensity;
- Filters the signal to eliminate noise;
- Detects observed microstructural features (porosities) from a grey level intensity threshold.

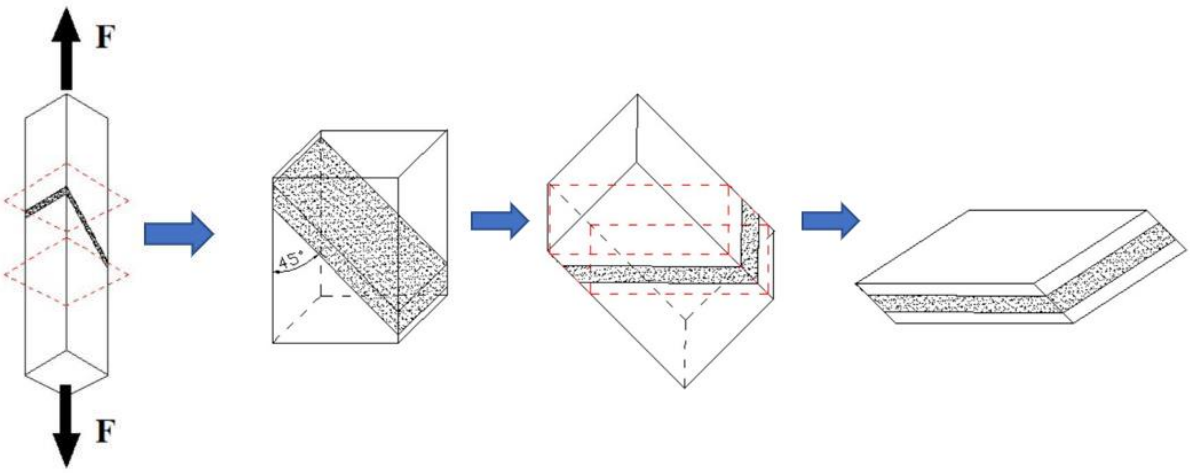

Figure 6. Schematic representation of the central part of the reconstructed sample

This processing tool was therefore developed in this study to enable the operator to automatically detect the required microstructural features from the raw signal shown as an example in Figure 8b (the signal representing the grey levels along a path for the image in Figure 8a).
Therefore, to extract the mean intensity I_0 present in the raw images, a calculation method based on the simulation of the characteristics of a real synthetic volume has been developed. The method will be used to analyse the raw data obtained and examine it in order to separate the porosities initially generated. This is possible using Matlab software.
The generation of the synthetic volume allows the calculation and extraction of the average intensity in the form of a polynomial equation with two unknowns, which allows the analysed image to be treated as a whole.
The real data is then analysed using the same principle to extract the average intensity and separate the porosities using Otsu method [14].

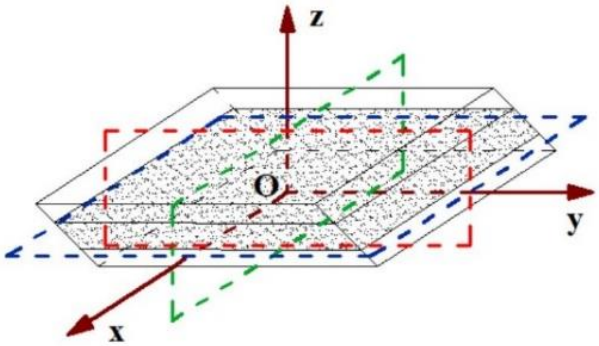

a) Schematic representation of the central part of the reconstructed sample

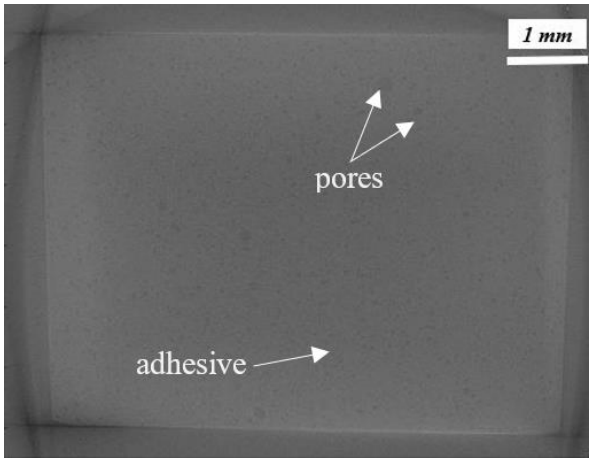

b) Slice xOy in the middle of the adhesive

c) Slice yOz in the middle of the adhesive

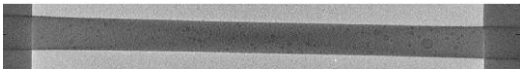

d) Slice xOz in the middle of the adhesive

Figure 7. Reconstructed volume of the sample

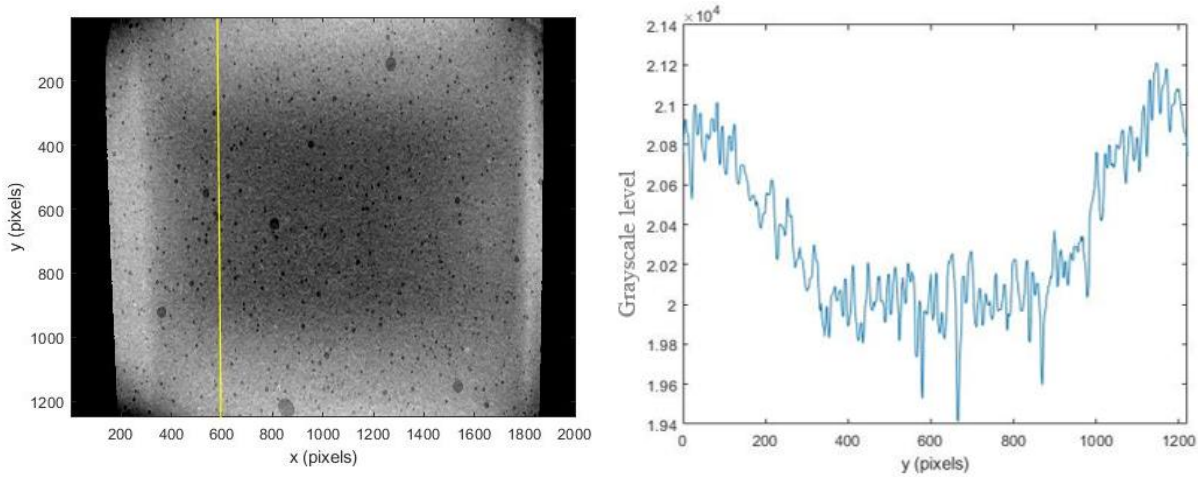

a) Slice in the middle of the adhesive b) Grayscale along a path (yellow line on a))

Figure 8. A slice of raw data

RESULTS OF POROSITY ANALYSIS

The X-ray tomography images obtained for specimens subjected to tensile-shear loads (Figures 7b to 7d) are difficult to analyse. Due to the large size of the reconstituted volume, these samples could not be analysed directly. It was necessary to cut out the central part of the sample containing the adhesive and a small part of the substrate (Figure 6). The resulting volume was shown schematically in Figure 7a. Next, this volume will be analysed and an attempt will be made to find the porosities using the processing tool developed.

Separating the adhesive from the substrates and ambient air was the first challenge. The Figure 7d shows that the adhesive volume obtained has a slight inclination. Using ImageJ software [6], the volume was rotated to make it horizontal in order not to interfere with subsequent analysis. Figure 9a shows, as an example, an upside-down cut of the middle of the adhesive. For a better view, the scale has been increased vertically.

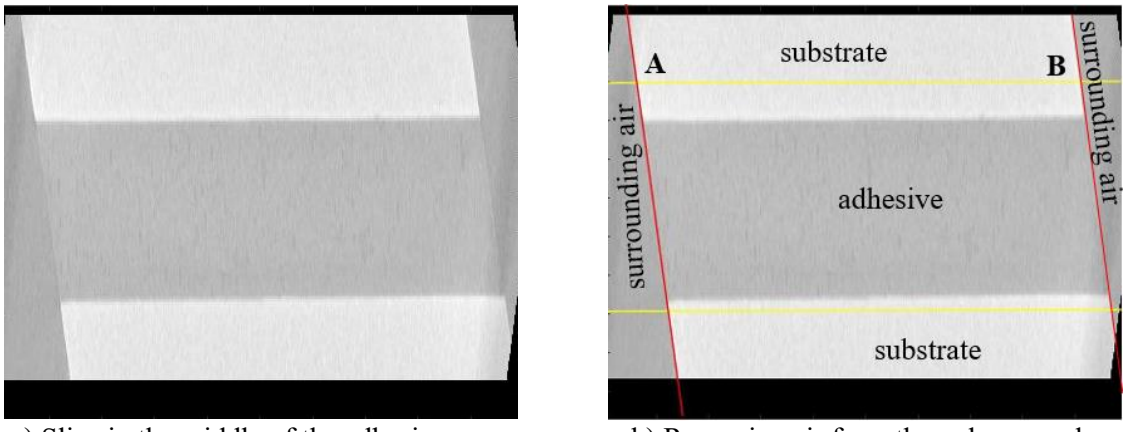

a) Slice in the middle of the adhesive b) Removing air from the volume analysed

Figure 9. Slice in the raw volume

The high noise and medium intensity of the raw images do not allow us to separate the three phases using simple methods such as the Otsu method. Thus, the method used to separate the air around the sample consists in finding two linear equations that describe the sample edges. The method is based on identifying two or more points on the sample contour by which we can describe these equations. This is achieved by deriving grayscale values along certain trajectories that cross the image on the x-axis in the areas where the substrate is located.

For the analysed image (Figure 9b), we have marked the selected trajectories with two yellow lines. The derived signal corresponding to one of these trajectories is shown graphically in Figure 10a, where the peaks corresponding to points A and B in the analysed image can be seen (Figure 10b).

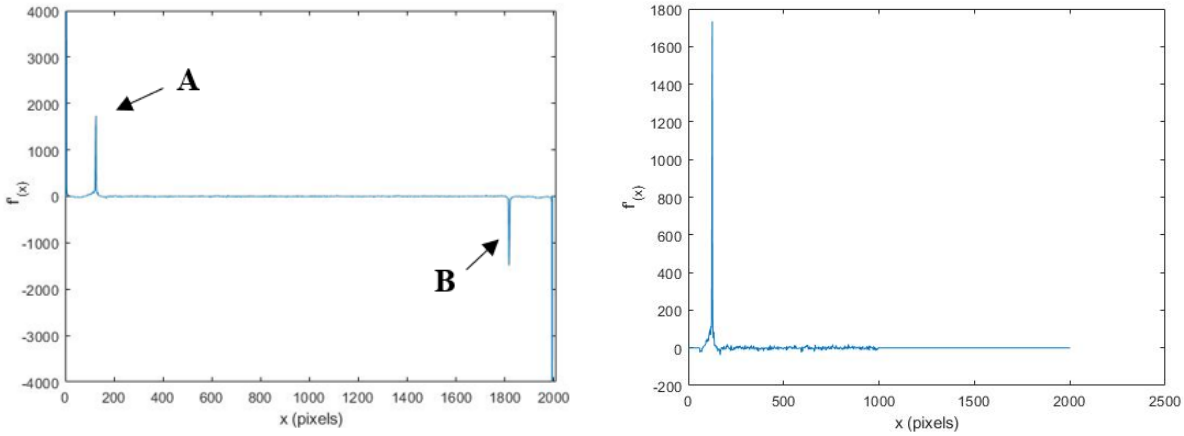

a) Derived signal

b) The signal at the boundary between air and substrate

Figure 10. Identification of points at the boundary between air and substrate

The peaks are isolated and located so that the equations corresponding to the boundary between the ambient air and the substrate can be identified. Using Matlab, we identified the two equations of the form $f_{(x)} = ax^2 + bx + c$, whose graphical representation is shown in Figure 9b by the two red lines. For each image, the greyscale values that lie between the two equations are retained, the others are set to 0. An image similar to Figure 11 is obtained, in which the adhesive and a part of the substrate are retained.

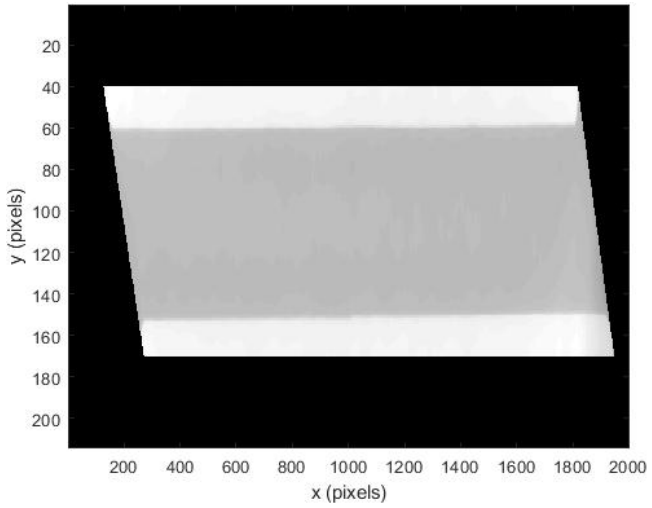

Figure 11. Slice in raw volume without air

In the resulting image (Figure 11), the contrast between the grayscale values corresponding to the substrates and the adhesive is clear. In this case, the separation of the substrates from the adhesive is carried out using the histogram obtained and the threshold calculated according to the Otsu method shown in Figure 12. The image shown in Figure 13 results from the separation of the adhesive substrates. By processing this image, we created a mask, which we used to isolate the adhesive.

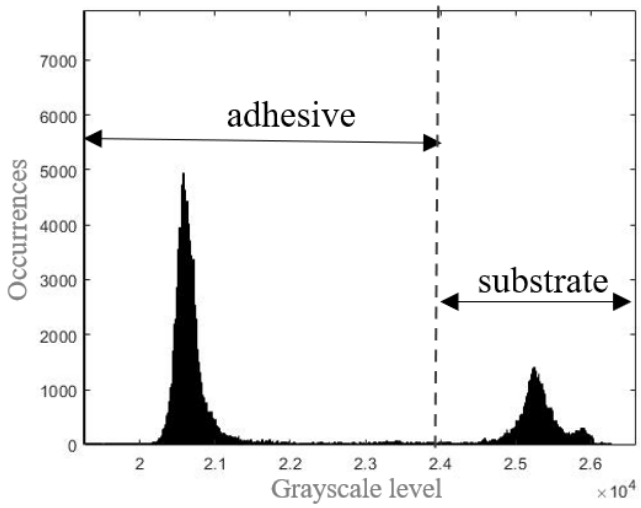

Figure 12. Histogram of volume and threshold calculated using the Otsu method

The mask (Figure 14) is multiplied by the raw volume to obtain the volume to be analysed without losing the information obtained by tomography. A volume of adhesive without ambient air or substrate is then obtained and subjected to analysis (Figure 15). To optimise analysis time, the resulting volume will be rotated by 90º using ImageJ software. Using scans in the xOy plane (Figure 16), the number of sections to be analysed will be reduced from 2,000 to 200, 80 of which are adhesive only.

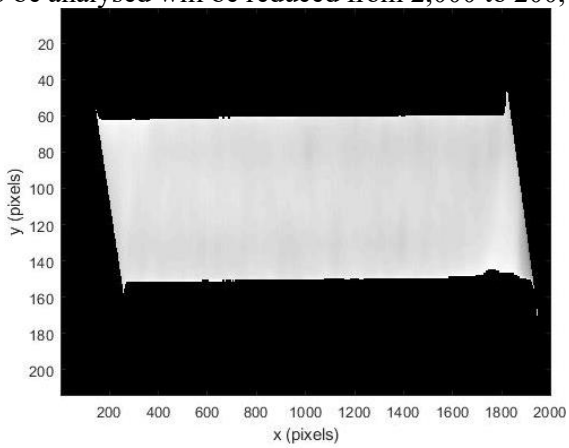

Figure 13. Removal of substrates by the Otsu method

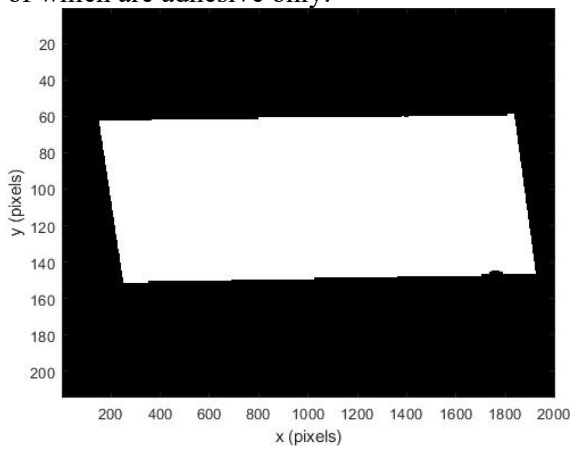

Figure 14. The mask

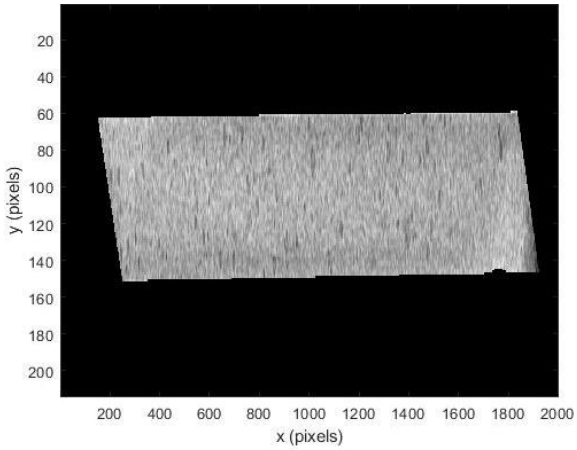

Figure 15. Slice through the obtained volume

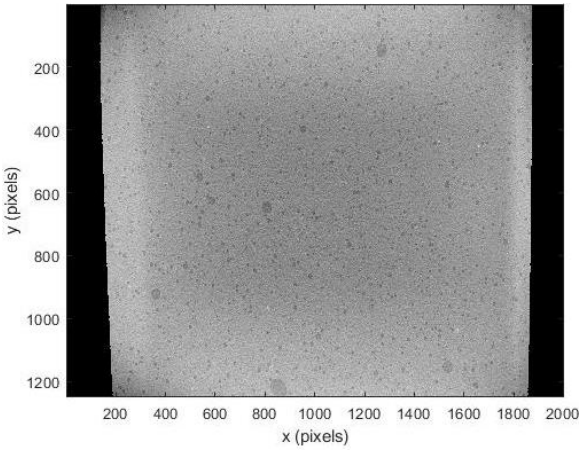

Figure 16. Slice through the obtained volume and rotate

After separating the adhesive volume, each image is analysed using the developed tool. In this case, the average intensity and noise are very significant, as shown in Figure 17, which shows a raw image (Figure 17a) and the signal corresponding to a randomly chosen trajectory (Figure 17b). The image obtained after extraction of I_0 is shown in Figure 18a. The signal corresponding to the previously chosen trajectory (Figure 18b) shows that the result is satisfactory and that we can therefore find the porosities in the adhesive.

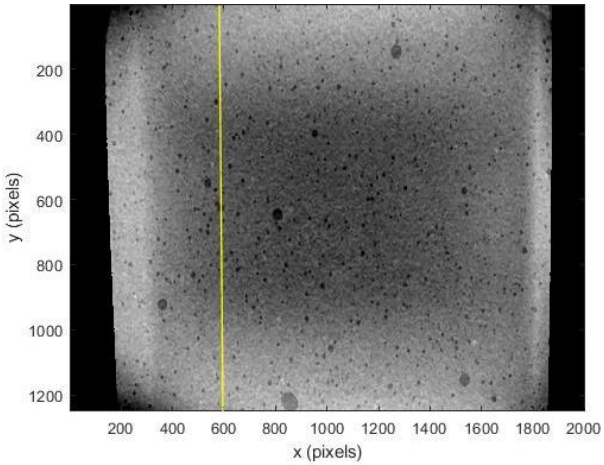

a) Unprocessed xOy slice in the middle of the adhesive

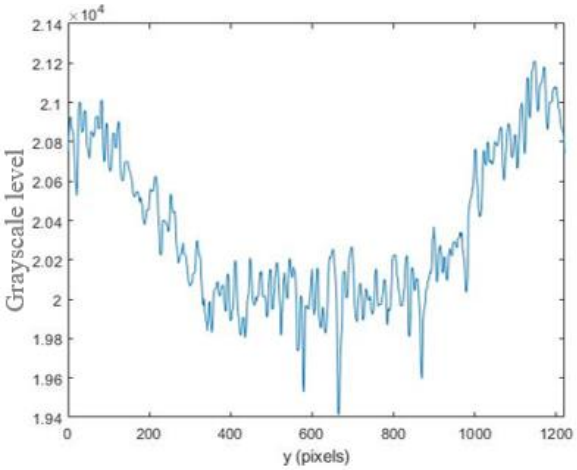

b) Grayscale values along a path (yellow line on a))

Figure 17. Slice in the raw volume

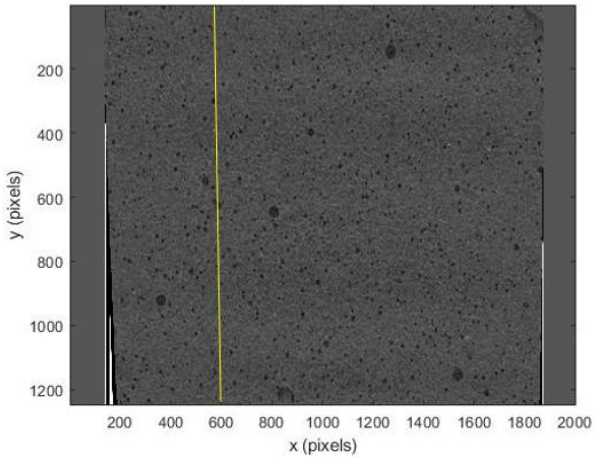

a) xOy slice in the middle of the adhesive

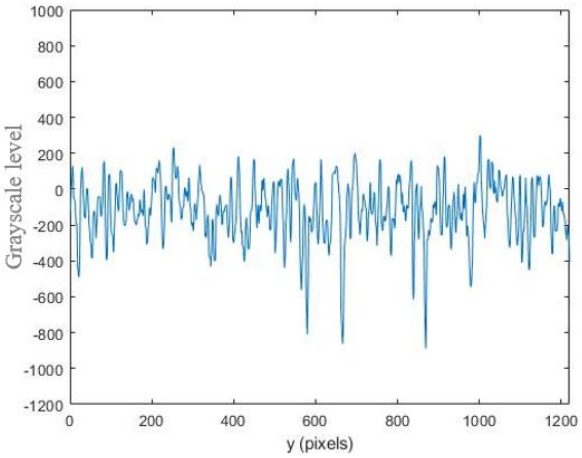

b) Grayscale values along a path (yellow line on a))

Figure 18. Slice in the raw volume after extraction of I_0

Therefore, by using the developed tool, we were able to extract the mean intensity and then separate these porosities from the adhesive using the Otsu method. For example, the image in Figure 19b shows the porosities in the image in Figure 19a (image obtained after extraction of I_0). The shape and number of porosities can be easily distinguished, allowing us to perform quantitative analysis of these porosities.

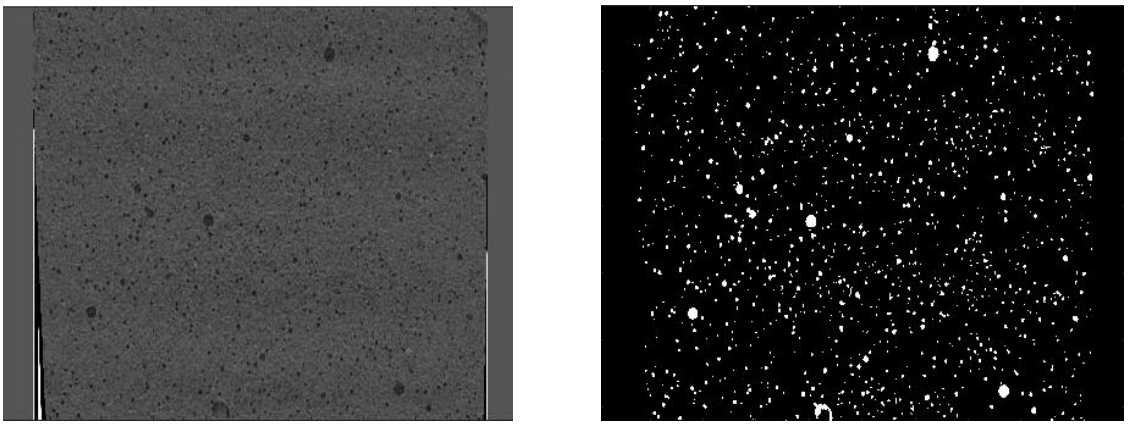

a) Slice in the middle of the adhesive b) Porosities

Figure 19. Slice in the raw volume

The sample analysed in the case of tensile-shear stress was loaded 7 times at 170 N each until failure (Figure 5). The differences between the porosities found in the sample at the initial stress state and before failure can be seen in Figure 20. Comparing Figure 20a with Figure 20b, we can see a significantly increase in porosity density as the applied force increases. By dividing the two porosity volumes shown in Figures 20a and 20b, we obtain the images shown in Figures 21a and 21b.
The increase in the size and number of porosities is clearly visible in these images, and comparison of these cross-sections allows us to deduce a visible transverse contraction of the pores (in the direction of the arrows in Figure 21b). In addition, a very interesting observation for the section in Figure 21b is the appearance of an interface break between the substrate and the adhesive (marked in red on the Figure 21b).

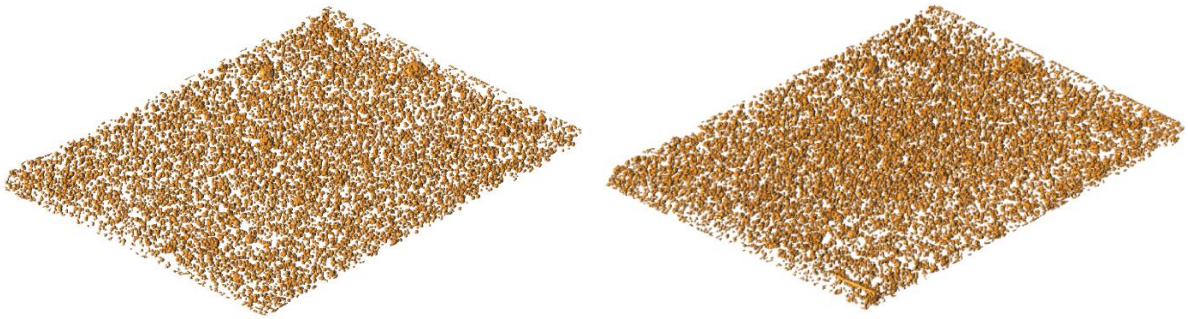

a) Porosities at initial stress state b) Porosities at final load before failure

Figure 20. Porosities found in the volume of adhesive

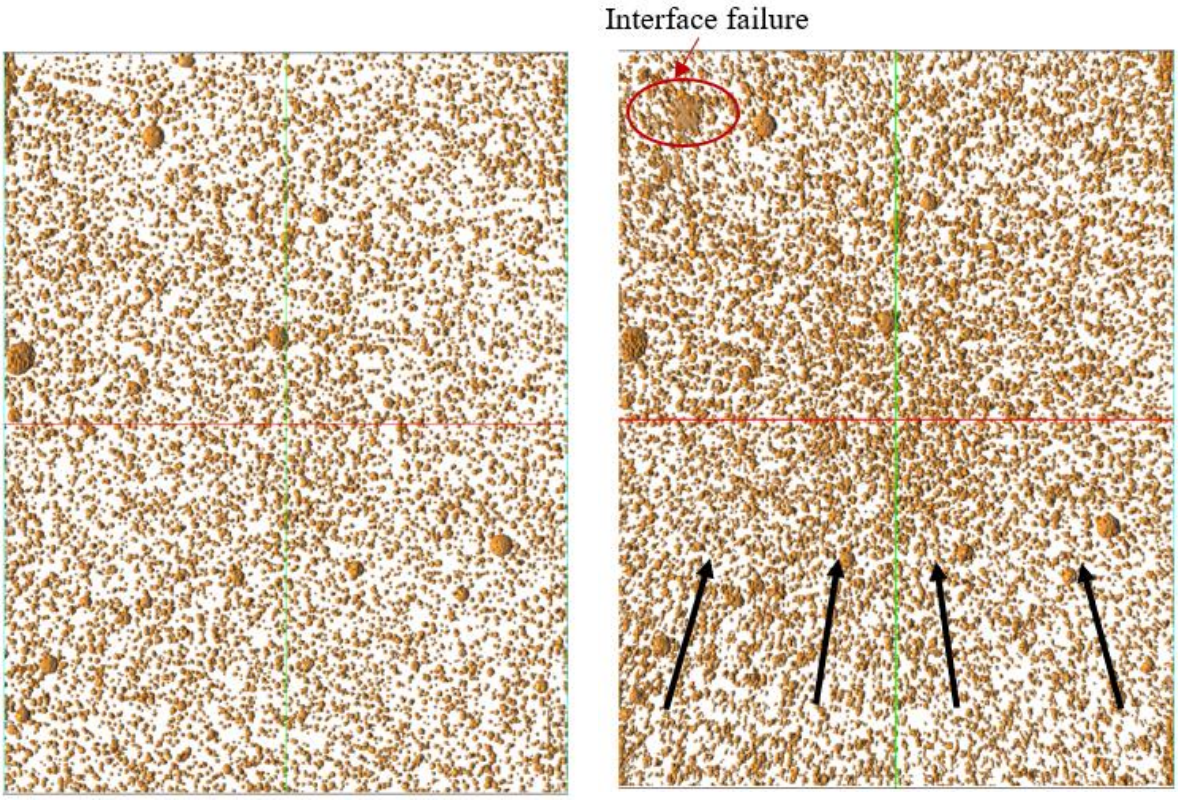

a) Porosities at initial stress state b) Porosities at final stress state before failure

Figure 21. Comparison of the porosities in a slice of the adhesive joint under tensile-shear stress

The graph in Figure 22 shows the increasing evolution of the number of pores with increasing load applied to the sample. The constant increase in the number of pores and then its decrease as the load exceeds around 850 N can be interpreted as a coalescence of porosity.
The evolution of the relative volume fraction of the porosity as a function of the applied load is illustrated in Figure 23 which is directly proportional to the load. The consistency of the increase in overall porosity size confirms the assertion that the number of porosities has increased to some extent, as observed in Figure 22, and that some of them have fused to create larger porosities.
An important result is the evolution of porosity distribution as a function of applied force (Figure 24). The increase in the number of porosities and the increase in their diameter can be seen as a visible difference between the histograms plotted for the first (ep9 00) and last (ep9 07) loading before sample breakage.
This result shows that the proposed formulation for the analysis of adhesive porosity is related to the force applied throughout the test. One of the main advantages of this approach is that it is parameterizable in the sense that, a priori, it only requires adaptation of the volumes analysed by the adhesive in the bonded joints.

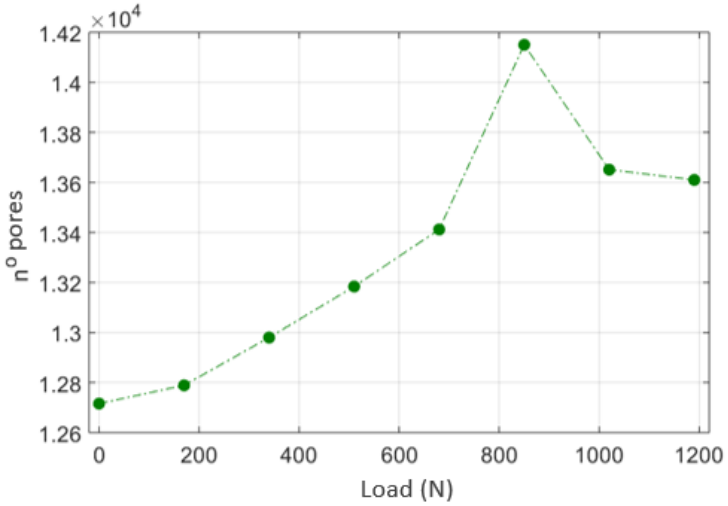

Figure 22. Evolution of total porosity versus load level

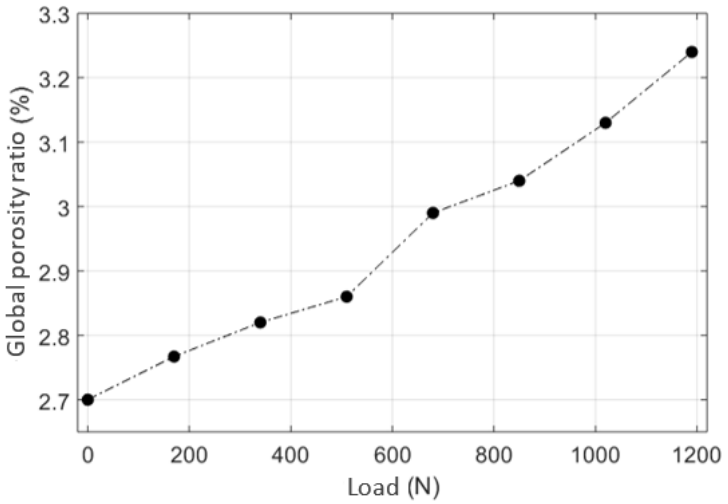

Figure 23. Evolution of the relative volume fraction of porosity versus load level

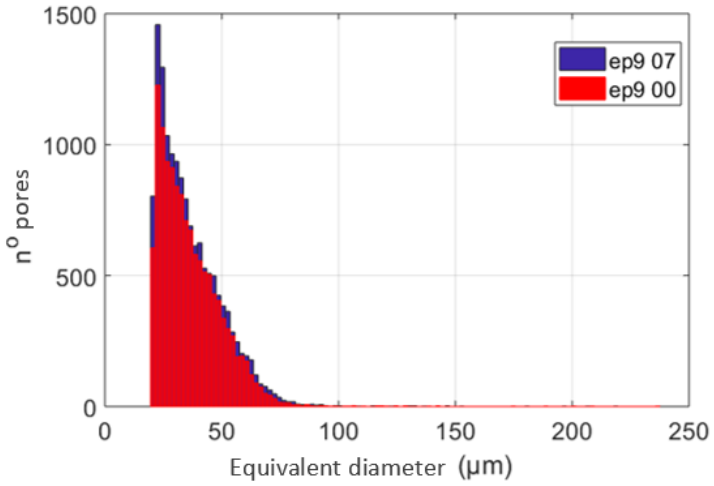

Figure 24. Distribution of the pores versus equivalent diameter

CONCLUSIONS

The aim of this paper was to post-process in-situ tests to characterize the porosity distribution of the adhesive joint using X-ray µ-tomography, and to analyse the evolution of this distribution during mechanical loading of the joint. Depending on the load applied, several parameters were recovered, such as porosity size, number and geometric shape.
The study of the effect of defects on the mechanical behaviour of bonded joints involves performing fracture tests on model specimens to which stresses representative of those experienced by the structure are applied. Beforehand, the behaviour of the adhesive joint was characterised by tensile-shear stress tests carried out on specific specimens. Therefore, these specific models were then explained, with regard to the preparation of the samples used in the tests, as well as the experimental conditions applied. This was followed by an explanation of how the X-ray tomography data was recovered for analysis. At the same time, we identified the importance of developing a tool to study the data in order to examine and analyse the pores present in the adhesive, which is able to extract the average intensity from the analysed images.
The raw data was then analysed using the same principle to extract the mean intensity and separate the porosities using the Otsu method. Finally, a volume of binary images was obtained in which the shape and number of porosities could be clearly distinguished. The location of the porosities allowed us to carry out a quantitative analysis. This analysis revealed an increase in the size and number of porosities as the applied force increased.
An interesting result was observed by examining the evolution of the number of porosities as a function of the force applied, namely the onset of porosity fusion after a certain stress threshold. In the same case, a break at the interface between the adhesive and the substrate was observed in the images corresponding to the last loads. This provides useful information about the imminent failure to occur.
In perspective, the first consideration is that the processing tool developed can be adapted and used for porosity analysis both for adhesive testing (as in our case) and for several types of material. Having the advantage of being parameterizable, this processing tool can be easily integrated into complex numerical calculation models. These calculation models can be used to determine the evolution of the mechanical behaviour of an adhesive joint and could also be used to anticipate and prevent the degradation of the material analysed.
Finally, thanks to this work, the method designed can be used to study the influence of porosity on an adhesive joint and implicitly on the mechanical behaviour of assemblies subjected to different types of mechanical stress.

REFERENCES

[1] Alfonso, L., Badulescu, C., Carrere, N. (2018). Use of the modified Arcan fixture to study the strength of bonded assemblies for automotive applications: effect of different parameters, *In: Journal of Adhesion and Adhesives, Volume 80*, pages 104–114

[2] Ilioni, A., Le Gac, P.Y., Badulescu, C., Thévenet, D., Davies, P. (2017). 22. Prediction of mechanical behaviour of a bulk epoxy adhesive in a marine environment, *Journal of Adhesion*, https://doi.org/10.1080/00218464.2017.1377616

[3] Salvo, L., Suéry, M., Marmottant, A., Limodin, N., Bernard D. (2010, November–December*).* 3D imaging in material science: Application of X-ray tomography, *Comptes Rendus Physique, Volume 11, Issues 9–10,* pages 641–649

[4] Bouterf, A. et al. (2017). Identification of the Crushing Behavior of Brittle Foam: From Indentation to Oedometric Tests. *Journal of the Mechanics and Physics of Solids, Volume* 98, pages 181–200. ..3

[5] Buffiere, J-Y., Marie, E., Adrien, J., Masse, J.P., Boller, E. (2010). *In Situ* Experiments with X ray Tomography: An Attractive Tool for Experimental Mechanics, *Experimental Mechanics, Volume 50,* pages 289–305

[6] http://rsbweb.nih.gov/ij. Consulté le 15/05/2019

[7] www.vsg3d.com. Consulté le 15/05/2019

[8] www.volumegraphics.com. Consulté le 15/05/2019

[9] Youssef, S., Maire, E., Gartner, R. (2005). Finite element modelling of the actual structure of cellular materials determined by X ray tomography, *Acta Mater, Volume 53*, pages 719 –730

[10] Dumont, V. (2020). On the durability of structural adhesive bonds in thermal environments: application to space-oriented optical systems. *PhD thesis.*

[11] Dumont, V., Badulescu, C., Adrien, J., Carrere, N., Maire, E. (2019). Experimental Investigation of Porosity in a Bonded Assembly by means of X ray Tomography and Microscopic Observations. *The Journal of Adhesion Volume 97(6), Issues 1-25*

[12] Lesseur, J (2015). *Imagerie 3D des matériaux et modélisations numériques : application aux multimatériaux ferroélectriques. Matériaux. Université de Bordeaux*, Consulté le 20/06/2019 à https://tel.archives-ouvertes.fr/tel-01281311

[13] Chan, T. F., Vese, L. A. (2001). Active contours without edges. *IEEE Transactions on Image Processing, Volume 10, Issue 2*, pages 266-277

[14] Otsu, N. (1979). A Threshold Selection Method from Gray-Level Histograms. *IEEE Transactions on Systems, Man, and Cybernetics 9.1*, pages 62-66